



Experimental study of flash evaporation of a water film

D. Saury *, S. Harmand, M. Siroux

Laboratoire de Mécanique et Énergétique, Université de Valenciennes et du Hainaut Cambrésis, Le Mont Houy, 59313 Valenciennes Cedex 9, France

Received 23 July 2001; received in revised form 26 October 2001

Abstract

This experimental study of the flash evaporation phenomenon of a water film was carried out with an initial water height of 15 mm, superheats ranging from 1 to 35 K and initial temperatures from 30 to 75 °C. During a sudden pressure drop, temperature measurements of the water film allowed us to determine the water mass evaporated by this phenomenon as well as the mass flow rates. A correlation between the water mass evaporated by flashing and the superheat was then obtained. Evolution of the flash evaporation rate coefficient let us estimate the duration of the flash evaporation phenomenon. © 2002 Elsevier Science Ltd. All rights reserved.

Keywords: Flash evaporation; Saturation temperature; Evaporation coefficient; Superheat

1. Introduction

When a liquid is exposed to a sudden pressure drop below its saturation pressure, all the heat cannot be contained in the liquid as sensible heat, and the heat surplus is transformed into latent heat of vaporization. This is at the origin of the formation of vapor bubbles inside the liquid bulk: it is the so-called flash evaporation or flashing phenomenon, resulting in a temperature drop of the liquid.

Flash evaporation is used in processes of steam generation such as water desalination. There are also other fields of application for the flash evaporation phenomenon such as the deposit of a thin layer of materials on a surface [1], or the drying of sterile loads in the vapor sterilization processes. Aoki [2,3] studied heat flux exchange due to the water flash evaporation under low pressure conditions. His study dealt with the cooling of a hot cylindrical surface by pulverized water. He showed that the flash evaporation which occurred when pulverized water reached the hot surface, had a high

heat-rejection capacity per unit coolant mass. If we add to this the safety of using water as a cooling agent, we can easily understand why the flash evaporation under low pressure is of great interest in spacecraft applications related to the cooling of the hot parts of a shuttle. Flash evaporation is a very quick phenomenon caused by an abrupt pressure drop which transforms the initially supercooled liquid bulk into superheated fluid. The phenomenon is initially very significant at the surface and forces the liquid to take on very heterogeneous temperature profiles, composed of superheated, saturated and subcooled areas. A significant turbulence perpetuates the flashing phenomenon, and involves mass transfer rates up to 10 or 12 times superior to those due to evaporation following the Fick law [4]. The absence of dissolved gas inside the liquid means that the flashing phenomenon only occurs at a surface level. After a relatively short time, the cooled liquid volume behaves in a similar way to a fluid undergoing an evaporation according to the Fick law.

Flashing is a process which gives rise to a vaporization flow rate more significant than that obtained during simple evaporation. It is necessary to have a better understanding of it in order to apply it wisely. With this objective in mind, experimental apparatus was put together in our laboratory, in order to study this phenomenon in more detail, and analyze the evolution of

* Corresponding author. Tel.: +33-3-2751-1987; fax: +33-3-2751-1961.

E-mail address: Didier.Saury@univ-valenciennes.fr (D. Saury).

Nomenclature

A	horizontal cross-sectional area of flash chamber [m ²]
C	salt concentration [%]
c_p	specific heat of liquid [J/kg K]
d	flash chamber diameter [m]
H	height of liquid [m]
h_{fg}	latent heat of vaporization [J/kg]
K	flash evaporation rate coefficient [s/m]
m	mass of liquid [kg]
m_0	initial mass of liquid [kg]
m_{ev}	evaporated mass of liquid [kg]
m_{ev}^f	final evaporated mass [kg]
\dot{m}_{ev}	instantaneous evaporated mass flow [kg/s]
p	flash chamber pressure [Pa]
p_0	initial pressure of container [Pa]
p_e	equilibrium pressure [Pa]
p_w	saturated vapor pressure [Pa]
t	time [s]
T	temperature of water [°C]
T_0	initial temperature of water [°C]

T_e	equilibrium temperature of water [°C]
t^*	flashing time [s]
t_0	delayed time of initiation of evaporation [s]
w	instantaneous evaporated mass flux [kg/m ² s]

Greek symbols

α_1	thermal diffusivity of liquid [m ² /s]
Δp	pressure drop [Pa]
ΔT	superheat [K]
ρ_l	density of liquid [kg/m ³]
ρ_v	density of steam [kg/m ³]
σ	surface tension [N/m]

Dimensionless numbers

Ja	Jacob number
NEF	non-equilibrium function
NEF*	non-equilibrium function at time t^*
p_{adim}	dimensionless pressure
Pr	Prandtl number of water

several characteristic parameters such as flashing time or evaporated mass.

2. Bibliographical synthesis

Key parameters influencing the water flash evaporation phenomenon have been given by several authors [4–8]. Of particular interest are superheat (due to the pressure difference): $\Delta T = T_0 - T_e$, initial temperature: T_0 , level of the liquid: H , and state of the fluid (supercooled or saturated).

To study water flash evaporation, dimensionless numbers and other parameters giving a good idea of flashing phenomenon were introduced. These various parameters are described below.

2.1. Non-equilibrium function (NEF)

Miyatake et al. [5,6] studied flash evaporation of water films 100, 196, 200 and 225 mm high. Equilibrium temperatures of water ranged from 40 to 80 °C, superheats from 2.5 to 5.5 K, for a range of equilibrium pressure from 74 to 463 mbar. In this study, Miyatake et al. [5,6] introduced the dimensionless number NEF. This number characterized the evolution of temperature during the flashing phenomenon

$$NEF(t) = \frac{T(t) - T_e}{T_0 - T_e}. \quad (1)$$

Miyatake also defined dimensionless pressure by

$$p_{adim}(t) = \frac{p(t) - p_e}{p(0) - p_e}. \quad (2)$$

Fig. 1 gives an example of the NEF evolution versus time based on Miyatake's data. This graph shows a very strong slope followed by a more gradual one. Intersection of these two slopes gives what we call the flashing time t^* as well as the NEF at time t^* called NEF*. Miyatake proposed a correlation between t^* , equilibrium temperature T_e and superheat ΔT [5]

$$t^* = 44 T_e^{-0.86} \Delta T^{0.55}. \quad (3)$$

He also suggested a link between NEF at time t^* (NEF*), equilibrium temperature and superheat.

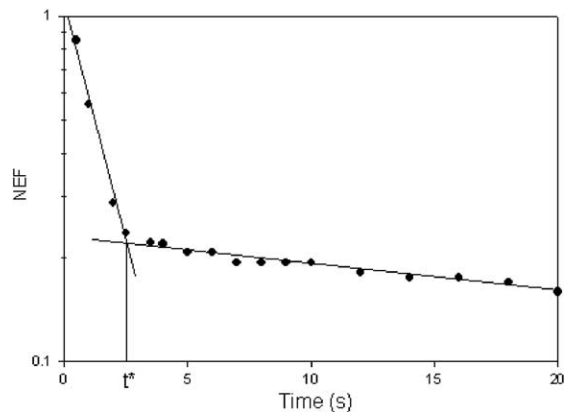


Fig. 1. Miyatake's typical NEF evolution versus time.

Table 1
Summing up of the main flashing parameters values

	Miyatake et al. [5]	Miyatake et al. [6]	Gopalakrishna et al. [7]	Kim and Lior [8]	Our study
T_e (°C)	40–80	40–80	–	–	–
T_0 (°C)	–	–	25–80	40–80	30–75
ΔT (K)	3–5	2.5–5.5	0.5–10	2–7	1–35
H (mm)	196–225	100, 200	165, 305, 457	380	15
p_0 (mbar)	73–473 ^a	73–473 ^a	30–310 ^a	66–354 ^a	50, 100, 150, 200

^a These estimated values are based on the initial temperature and superheat values or equilibrium temperature given by the authors.

$$NEF^* = \frac{T(t^*) - T_e}{T_0 - T_e}, \tag{4}$$

$$NEF^* = \frac{1}{1 + 2.8 \times 10^{-3} T_e^{1.3} \Delta T}.$$

Furthermore, Miyatake et al. [5] put forward the following equation connecting NEF to NEF*, t and t^*

$$\frac{\ln NEF(t)}{\ln NEF^*} = \frac{t - t_0}{t^* - t_0} \tag{5}$$

with t_0 : delayed time of initiation of evaporation.

From Eqs. (3) to (5), we can deduce an equation between NEF, time t , T_e and ΔT .

$$NEF = [1 + 2.8 \times 10^{-3} T_e^{1.3} \Delta T]^{-((t-t_0)/(44 \times T_e^{-0.86} \Delta T^{0.55} - t_0))}. \tag{6}$$

2.2. The flash evaporation rate coefficient: K

By considering pressure difference – between saturation pressure p_w at the mean temperature of liquid and equilibrium pressure p_e – as the driving force for flash evaporation, we can define the flash evaporation rate coefficient by

$$K = \frac{w(t)}{p_w - p_e} = \frac{\dot{m}_{ev}}{A(p_w - p_e)}, \tag{7}$$

where $w(t)$ is the instantaneous mass flux.

Miyatake et al. [5] noted that K is not time dependent, it is almost independent of superheat ΔT , but decreases when equilibrium temperature T_e increases. Later, a more extensive study of this coefficient was carried out by Miyatake et al. [6]. It confirmed previous results and showed that for $T_e \leq 75$ °C, K increased when the level of fluid decreased. On the other hand, for $T_e \geq 75$ °C, K increased when liquid level increased.

2.3. The mass evaporated by flashing

Gopalakrishna et al. [7] carried out experiments on water desalination for initial liquid temperatures ranging from 25 to 80 °C, a superheat from 0.5 to 10 K, a salt concentration from 0% to 3.5% and for distilled water

heights of 165, 305 and 457 mm. By measuring the liquid level with a cathetometer, they identified a correlation giving the water mass evaporated by flashing at every moment

$$m_{ev} = m_v C_1 Ja_p^{a_1} Pr^{a_2} \left(\frac{\Delta p}{H}\right)^{a_3} (1 + C)^{a_4} \times [1 - \exp(-p_2 t)] \tag{8}$$

with:

$$p_2 = C_2 Ja_p^{b_1} \left(\frac{\Delta p}{H}\right)^{1000(b_2/\tau)}, \quad b_1 = 0.133,$$

$$b_2 = -1.6, \quad Ja_p = c_p T_0 \Delta p \frac{(\rho_l/\rho_v) - (1/\rho_v)}{h_{fg}^2},$$

$$m_v = Ja AH \rho_l, \quad Ja = \frac{c_p \Delta T}{h_{fg}}, \quad \tau = \frac{(\sigma/\Delta p)^2}{\alpha_1},$$

$$C_1 = 0.8867, \quad C_2 = 0.27, \quad a_1 = 0.05,$$

$$a_2 = -0.05, \quad a_3 = -0.05, \quad a_4 = 0.06.$$

This correlation was valid for the range of following variables:

$$0.1116 \leq \frac{\Delta p}{H} \leq 2.615, \quad 1 \leq 1 + C \leq 1.035,$$

$$12 \leq Ja_p \leq 197, \quad 2.706 \leq Pr \leq 5.941.$$

We therefore conclude that studies available in the literature concern liquid heights from 100 to 457 mm, initial temperatures from 25 to 80 °C, and superheat from 0.5 to 10 K. These values are summed up in Table 1.

3. Experimental setup

Our experimental setup was designed to carry out experiments with a water height H of 15 mm, an initial temperature ranging between 30 and 75 °C and an initial pressure between 50 and 200 mbar which corresponds to a superheat between 1 and 35 K.

Fig. 2 shows the experimental setup used for our study of water flash evaporation. The bench is composed of a 316 l tank in which a vacuum is created (1) and a 2.2 l flash evaporation chamber (2) filled with distilled water. Both tanks are cylindrical and are made of

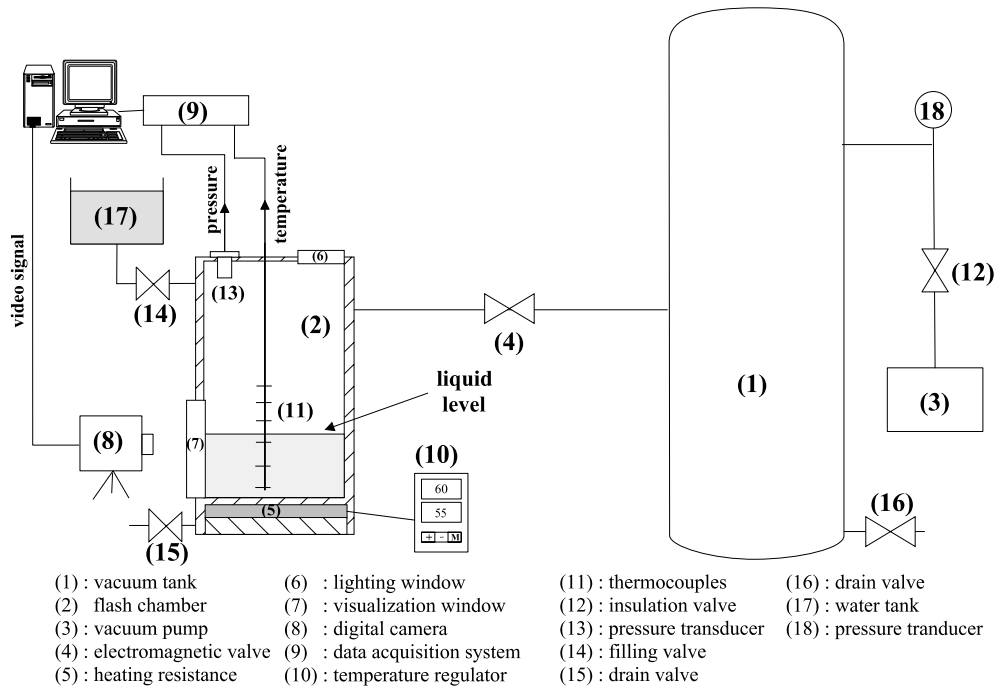


Fig. 2. Experimental setup of flash evaporation.

stainless steel. They are connected with a hand operated electromagnetic valve (4). The flash chamber has two windows: a visualization window in polycarbonate (7) and one which lets light in borosilicate (6). A heating power of 60 W (5), controlled by a temperature regulator (10) and stuck under the bottom of the evaporation container heats the water. Thermocouples (11) and a pressure transducer (13) in the chamber (2) make it possible to record temperatures as well as pressure inside the tank via a data acquisition system (9). Moreover, a digital camera (8) in front of the visualization window (7) records evolution of the flashing phenomenon with an acquisition frequency of 6 frames per second. The vacuum in the tank (1) is created using a liquid-ring pump (3) which goes up to 40 mbar absolutes with a flow rate between 0.2 and 0.4 m³/mn. A pressure transducer (18) at the input of the vacuum tank (1) controls pressure inside it.

3.1. Instrumentation

Liquid and vapor temperatures are measured by six type *T* thermocouples (copper–constantan) of diameter 0.08 mm (cf. Fig. 3). Type *T* was selected because of its good reaction to vacuum and humidity. It can measure temperatures from -270 to $+400$ °C, its precision is of 0.12 °C and its response time of 40 ms.

Pressure in the flash chamber (2) and vacuum tank (1) is measured by two pressure transducers. The first

one is a piezo-resistive sensor in stainless steel which measures absolute pressure on a 1.5 bar range. Its temperature range is from 20 to 100 °C. Its bandwidth is 13 kHz and its precision 1% of its measurement range. The second one is an active strain gauge. Its effective mea-

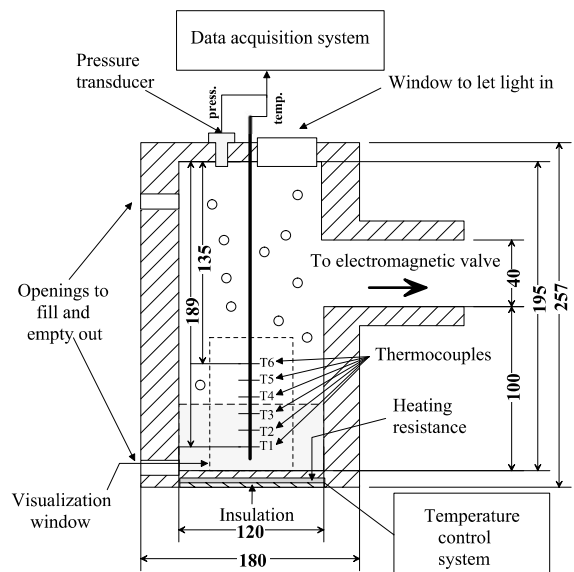


Fig. 3. Location of pressure and temperature gauges in the flash chamber.

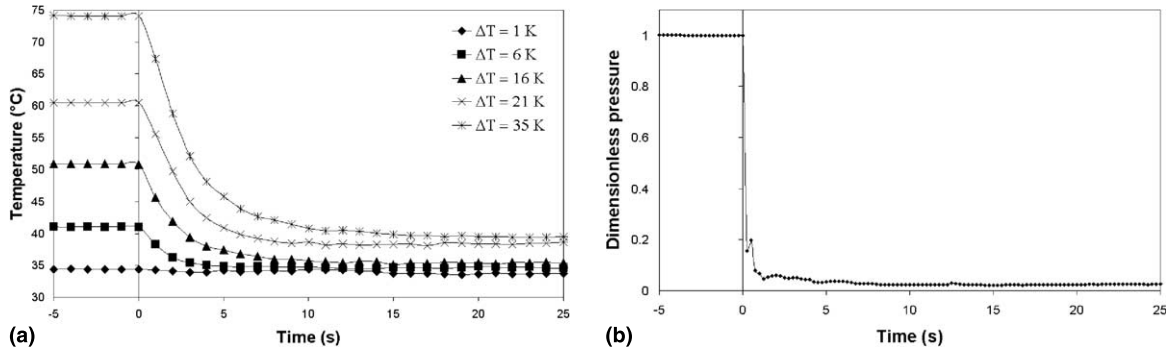


Fig. 4. Evolution of temperature (a) and dimensionless pressure (b) versus time for an initial pressure of 50 mbar.

surement range is from atmospheric pressure (1000 mbar) to 10^{-1} mbar. Its precision is $\pm 0.2\%$ of its measurement range.

The data acquisition system (HP75000B) is controlled by a PC via a HP-IB bus. Thermocouples are connected to this data logger using a HP-E1347A card and the connection between the pressure transducers and recorder is carried out by a HP-E1345A card.

3.2. Determination of evaporated mass and evaporated flow rate

The first step of an experimental test consists in lowering the pressure in the tank until the desired pressure level is reached. Then the flash chamber is filled with 169 g of distilled water in order to obtain a water height $H = 15$ mm. The liquid is then heated to the desired temperature with a heating resistance. The electromagnetic valve is then opened which causes contact between the vacuum tank and flash evaporation container. A data acquisition system records the evolution of the six thermocouples temperatures T_1 to T_6 , and the pressure in the flash chamber during the drop in pressure (cf. Fig. 3).

The evaporated mass flow rate is calculated from a heat balance on liquid bulk in the flash evaporation chamber. Thermal inertia of the flash chamber walls is such that energy exchanges with outside are deemed negligible. Moreover, the speed of the flash evaporation phenomenon and the slight evolution of the walls' temperature during it, make us think that energy supplied by walls during flashing is negligible when compared to the other terms of the equation balance. Thus, the energy released by the sudden temperature drop is completely used to vaporize a quantity $\delta m > 0$ of distilled water.

At one unspecified moment t , we can therefore write the following energy balance

$$(m - \delta m)c_p(T - dT) - mc_pT - \delta mh_{fg} = 0, \quad (9)$$

then, we obtain (neglecting second-order terms)

$$\frac{\delta m}{m} = \frac{c_p dT}{h_{fg} + c_p T} \quad (10)$$

In addition, physical properties of water are quasi-constant on our range of temperatures [9], and the water mass m in the flash chamber is obtained by integration of this latter equation.

$$m = \rho_l AH \frac{1 + (c_p/h_{fg})T}{1 + (c_p/h_{fg})T_0}. \quad (11)$$

From this we can deduce the instantaneous evaporated mass of liquid m_{ev} :

$$m_{ev} = m_0 - m, \quad (12)$$

$$m_{ev} = \rho_l AH \left[1 - \frac{1 + (c_p/h_{fg})T}{1 + (c_p/h_{fg})T_0} \right]. \quad (13)$$

Once the evaporated mass has been obtained, we can deduce instantaneous evaporated mass flow rate since

$$\dot{m}_{ev} = \frac{dm_{ev}}{dt} = -\rho_l AH \frac{c_p/h_{fg}}{1 + (c_p/h_{fg})T_0} \frac{dT}{dt}. \quad (14)$$

4. Results and analysis

In this article we present an experimental study of the flash evaporation of a water film. Experiments were carried out for a fluid height $H = 15$ mm, initial pressures of 50, 100, 150 and 200 mbar and initial temperatures ranging between 30 and 75 °C, which correspond to superheats ΔT from 1 to 35 K. Since the liquid level in the flash chamber was low, all underwater thermocouples were at the same temperature. Results are plotted using the thermocouple called T_1 in Fig. 3. Evolutions of the liquid temperature and the dimensionless pressure in the flash chamber versus time are presented in Fig. 4 for

experiments with an initial pressure of 50 mbar. For other experiments ($p_0 = 100$ mbar, $p_0 = 150$ mbar and $p_0 = 200$ mbar), liquid temperature and dimensionless pressure profiles are the same as those presented in Fig. 4.

4.1. Visualization

We filmed the flashing phenomenon with a digital camera. Fig. 5 shows, respectively, the experiment with $p_0 = 50$ mbar and $T_0 = 40$ °C ($\Delta T = 1$ K) and the experiment with $p_0 = 100$ mbar and $T_0 = 60$ °C ($\Delta T = 14$ K). Fig. 5(a) shows the flashing chamber before the

beginning of the phenomenon: hot liquid at $T_0 = 40$ °C is in a stable state. Fig. 5(b) corresponds to the moment when the electromagnetic valve is opened: the violence of the flashing phenomenon is visible and the fluid is completely disrupted. Fig. 5(c) shows the phenomenon two seconds after the opening of the electromagnetic valve: the fluid is boiling. Lastly, in Fig. 5(d) we can see the water at rest again post-flashing phenomenon. Figs. 5(e)–(h) show the flash evaporation phenomenon at the same time but for an initial pressure of $p_0 = 100$ mbar and an initial temperature of $T_0 = 60$ °C. Both pictures confirm that the violence of the flashing phenomenon increases when superheat increases.

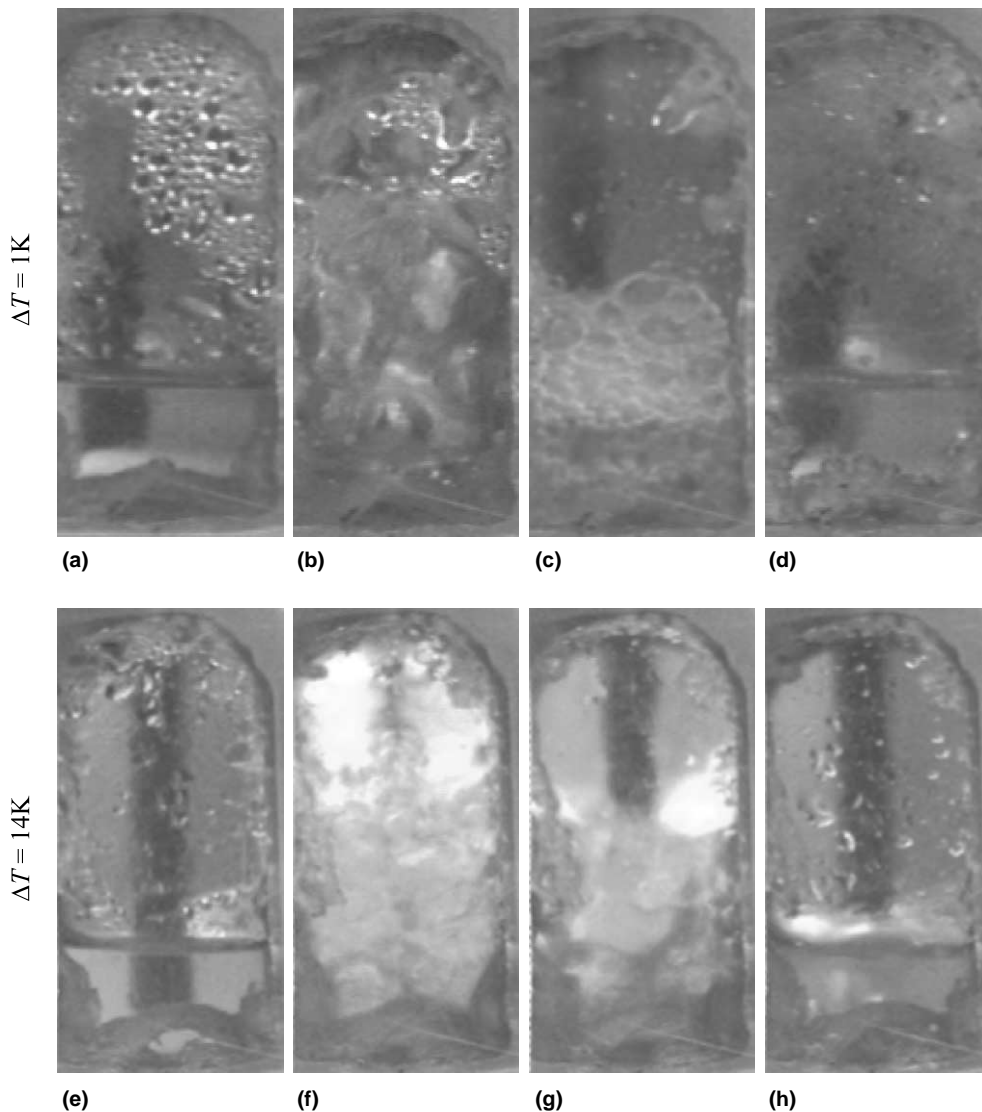


Fig. 5. Visualization of flash evaporation phenomenon: (a) $t = 0^-$; (b) $t = 0^+$; (c) $t = 2$ s; (d) $t = 5$ min; (e) $t = 0^-$; (f) $t = 0^+$; (g) $t = 2$ s; (h) $t = 5$ min.

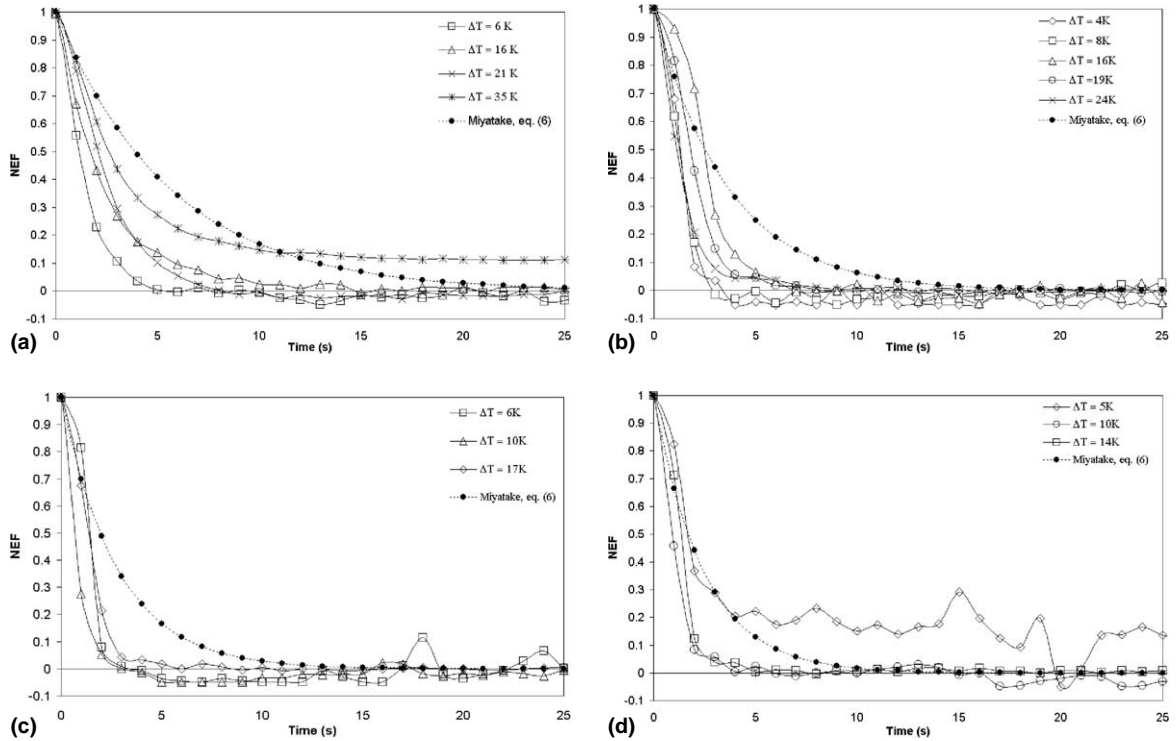


Fig. 6. Evolution of NEF versus time for different pressures: (a) $p_0 = 50$ mbar; (b) $p_0 = 100$ mbar; (c) $p_0 = 150$ mbar; (d) $p_0 = 200$ mbar.

4.2. NEF evolution

The graphs in Fig. 6 illustrate the evolution of NEF (Eq. (1)) versus time for various experimental setups. No matter which experiment is considered, we notice an exponential decay of this function with time. The NEF slope in the initial flashing period decreases with the initial pressure. For small superheats, NEF fluctuates significantly and sometimes negative values are obtained. This is due to the fact that after a relatively long time, the liquid temperature oscillates slightly around its equilibrium value T_e . This can be explained by the boiling phenomenon which slightly disturbs temperature measurements in the flash chamber and also by the additional energy which goes from the flash chamber walls to the liquid bulk.

Eq. (6) obtained by Miyatake and giving the evolution of NEF with time is valid for superheats ranging from 2.5 to 5.5 K, liquid heights between 100 and 225 mm, and initial pressures from 74 to 463 mbar. Results obtained with Eq. (1) ($t_0 = 0$ in our case) and our experimental results are compared in Fig. 6(a) for $\Delta T = 6$ K, Fig. 6(b) for $\Delta T = 4$ K, Fig. 6(c) for $\Delta T = 6$ K and Fig. 6(d) for $\Delta T = 5$ K. There is a significant difference between our experimental data and values given by Eq. (1). On the one hand, significant differences of liquid

level in our study ($H = 15$ mm) and in Miyatake's study ($100 \text{ mm} < H < 225$ mm) can explain these unequal results. On the other hand, the sudden pressure drop is not the same in our study and in Miyatake's which could also explain these differences.

Using the graphs in Fig. 6, we determined the flashing time according to the procedure described in Fig. 1 for each measurement, and we compared it with values obtained from the literature, and we compared it with values presented in Fig. 7. Eq. (3) was obtained by Miyatake for superheat values ranging between 2.5 and 5.5 K. As we

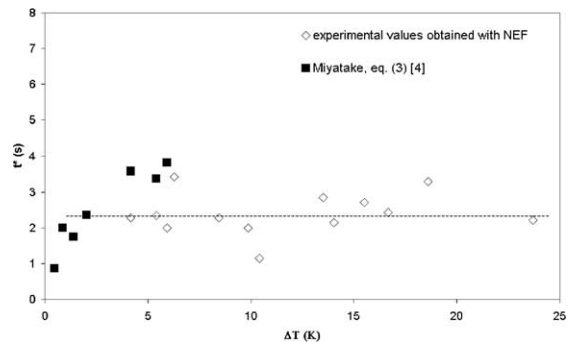


Fig. 7. Evolution of t^* versus superheat.

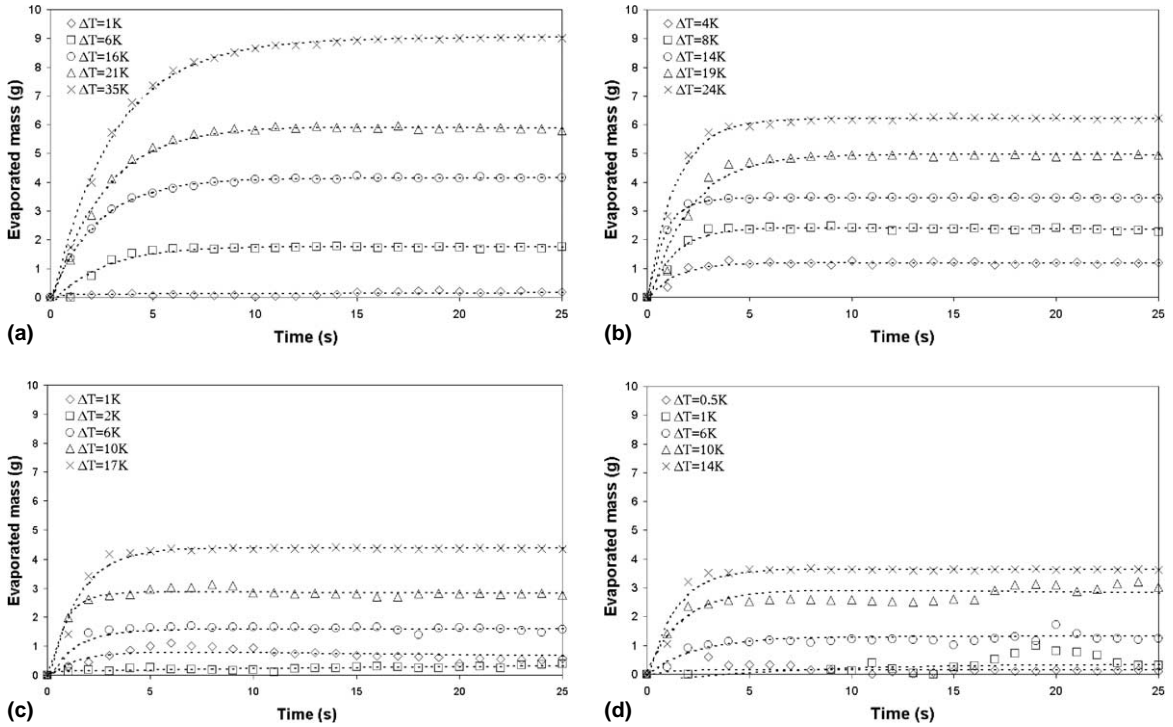


Fig. 8. Evolution of m_{ev} versus time for different pressures: (a) $p_0 = 50$ mbar; (b) $p_0 = 100$ mbar; (c) $p_0 = 150$ mbar; (d) $p_0 = 200$ mbar.

can see, values found for small superheats correlate rather well with those proposed by Miyatake’s formula. For more significant superheats, this formula cannot unfortunately be extrapolated. As far as our results are concerned, we note that broadly speaking t^* is not very dependent on superheat. However, uncertainty about t^* due to the method of determination itself does not make it possible to confirm this observation.

4.3. The mass evaporated by flashing

Use of formula (13) enables us to obtain graphs of evaporated mass with time which are presented in Fig. 8.

Mass evaporated by flashing evolves increasingly with time and tends towards a limit value after a while.

Fig. 9 shows the evolution of the limit value of the evaporated mass m_{ev}^f with initial pressure (Fig. 9(a)) and initial temperature of the liquid (Fig. 9(b)). The final flashed mass, m_{ev}^f , is a decreasing function of pressure and an increasing one of initial temperature.

In order to break away from this double dependence, we studied evolution of the final evaporated mass with liquid superheat for all experiments. Fig. 10 shows the results we obtained and confirms that evaporated mass is proportional to superheat. Indeed, the following empirical law is obtained

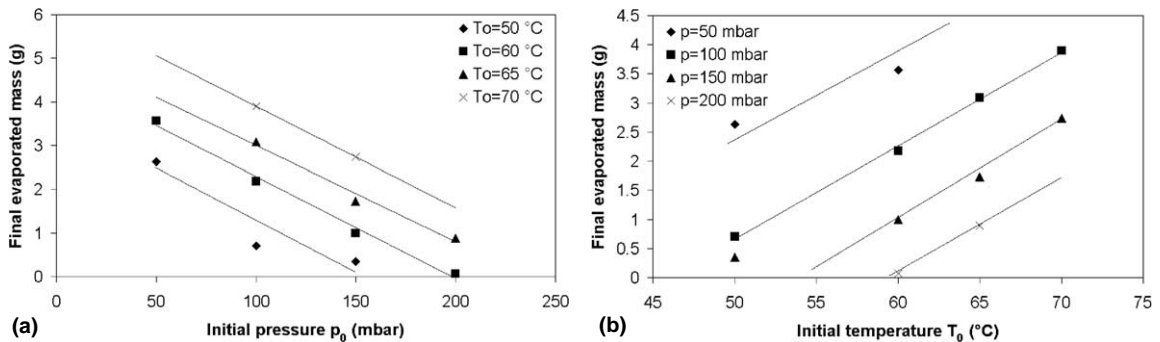


Fig. 9. Evolution of m_{ev}^f versus pressure (a) and initial temperature (b).

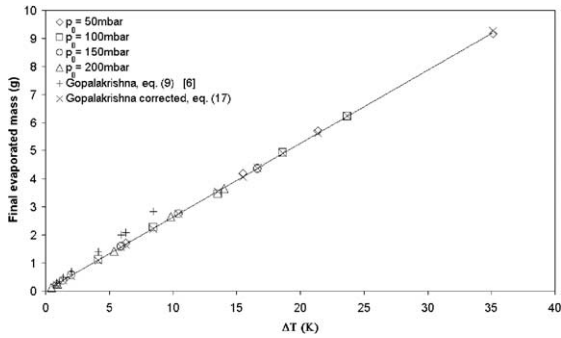


Fig. 10. Evolution of m_{ev}^f versus superheat.

$$m_{ev}^f = 0.2615 \Delta T. \quad (15)$$

We can also find this law analytically if we consider that the water mass variation in the chamber is negligible. This assumption is justified since evaporated mass in the chamber is small compared to the initial mass m_0 (<4%). Eq. (9) can therefore be rewritten as follows

$$m_0 c_p (T - dT) - m_0 c_p T - \delta m h_{fg} = 0, \quad (16)$$

so, we obtain

$$m_0 c_p \Delta T = m_{ev}^f h_{fg} \quad (17)$$

from which we deduce

$$m_{ev}^f = m_0 \frac{c_p}{h_{fg}} \Delta T = m_0 Ja. \quad (18)$$

In our case, $m_0 = 169$ g, so we obtain $m_0 \frac{c_p}{h_{fg}} = 0.2943$ g K⁻¹. This coefficient is close (10%) to the one obtained in our empirical law (15).

Eq. (8), given by Gopalakrishna, is valid for superheats from 0.5 to 10 K, a diameter of flash chamber $d' = 152$ mm, and significant water heights since we must have $0.1116 < \Delta p/H < 2.615$. This means that its formula cannot be used in our study where $39 < \Delta p/H < 48$ and where the flash chamber diameter is $d = 120$ mm. However, as it seems that the water level in the chamber slightly influences the flashing phenomenon, we compared the results of this correlation to our experimental data for $\Delta T < 10$ K. Fig. 10 plots the results obtained. The values of water masses evaporated by flashing obtained during our experimental measurements are slightly lower than those found with Eq. (8) and the relative error obtained varies between 15% and

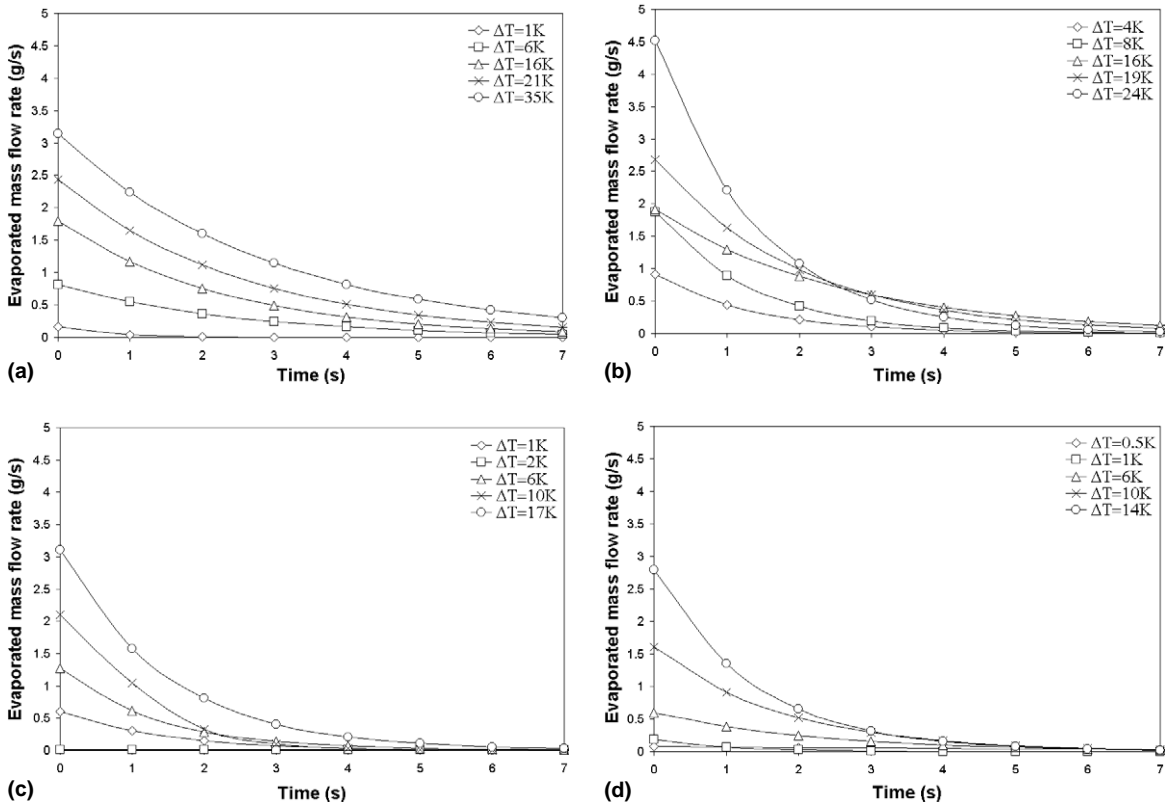


Fig. 11. Evolution of \dot{m}_{ev} versus time for different pressures: (a) $p_0 = 50$ mbar; (b) $p_0 = 100$ mbar; (c) $p_0 = 150$ mbar; (d) $p_0 = 200$ mbar.

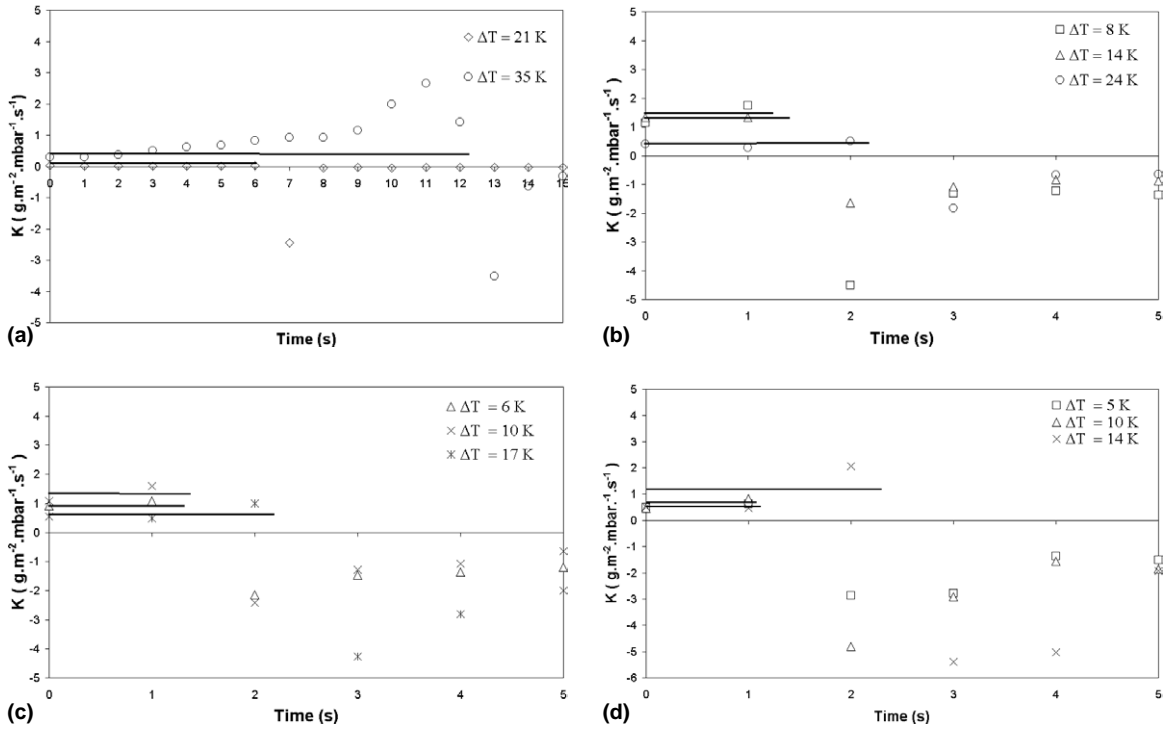


Fig. 12. Evolution of K versus time for different pressures: (a) $p_0 = 50$ mbar; (b) $p_0 = 100$ mbar; (c) $p_0 = 150$ mbar; (d) $p_0 = 200$ mbar.

23%. However, if the constant $C_1 = 0.8867$, experimentally obtained by Gopalakrishna and thus related to the geometry of his model, is corrected to take the diameter difference between our two experimental setups into account, we obtain a constant $C'_1 = C_1 \frac{120}{152} = 0.7$, and the maximum relative error obtained is now lower than 4%. As a result, a corrected Gopalakrishna's formula is obtained

$$m_{ev}^f = m_v C'_1 J a_p^{a_1} Pr^{a_2} \left(\frac{\Delta p}{H} \right)^{a_3} (1 + C)^{a_4} \quad (19)$$

with $C'_1 = C_1 \frac{d}{d'}$ where d corresponds to the diameter (in millimeter) of our flash chamber, and d' to Gopalakrishna's chamber [7].

Moreover, Fig. 10 shows that in our case formula (19) remains valid up to 35 K of superheat.

4.4. The instantaneous evaporated flow rate

After studying the evolution of the mass evaporated with time, we determined the instantaneous evaporated mass flow rate according to Eq. (14). Fig. 11 illustrates the evolution of this mass flow rate versus time as it decreases with time. Generally, this mass flow rate is an increasing function of superheat and a decreasing one of initial pressure.

4.5. Flash evaporation rate coefficient: K

Fig. 12 illustrates the evolution of the flash evaporation rate coefficient K versus time, obtained from Eq. (7). For a short period, which seems to correspond to the flashing time t^* , it is almost constant. However for longer times ($> t^*$), there is a significant oscillation and negative values are obtained which show the end of the evaporation phenomenon.

In Fig. 13, we plotted values of t^* obtained from the evolution of K (Fig. 12) and values obtained by Miyatake's method described in Section 2.1. Values obtained

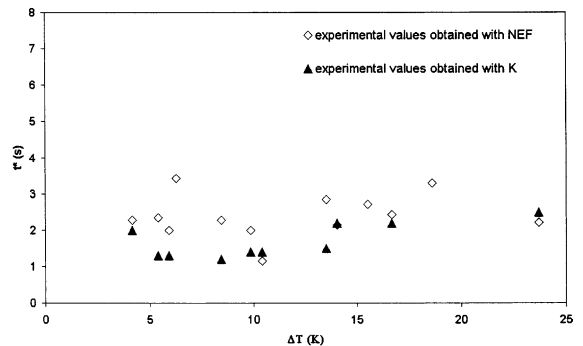


Fig. 13. Comparison between the two methods giving t^* .

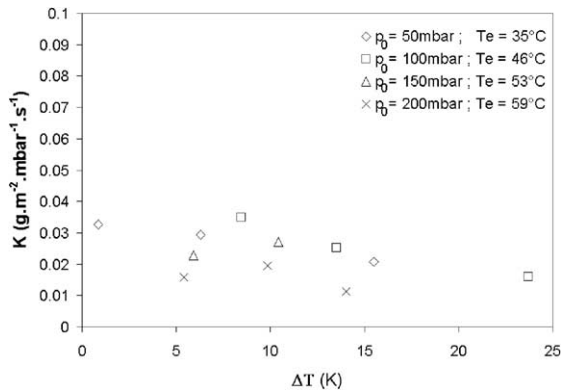


Fig. 14. Evolution of K versus superheat.

with this first method correlate rather well with those found with Miyatake's method. So, another way to determine this flashing time t^* seems to appear here.

Moreover, Fig. 14 which represents K versus superheat, illustrates that it is not after all very dependent on superheat. Once again this confirms Miyatake's results [5].

5. Conclusion

This article has described an experimental study concerning the flash evaporation of a water film. Experiments were carried out for an equilibrium temperature between 35 and 60 °C, pressures ranging between 50 and 200 mbar, and a water height of 15 mm. These experiments identified the parameters influencing the flash evaporation kinetic: namely the initial temperature of liquid and superheat. A relation of proportionality between the final mass of liquid evaporated by flashing and the superheat is proposed. In addition, we have shown that the factor of proportionality between the final mass of liquid evaporated and the superheat can be obtained from the heat balance in the flash chamber. Moreover, a method to determine flashing time starting from the flash evaporation rate coefficient has been put forward. This method seems to be in good agreement with the one proposed by Miyatake.

A new, larger, experimental apparatus is currently under construction at the laboratory. This should enable us to carry out experiments with a more significant water height and thus check the influence of the variation of the water level in the chamber on the kinetic of the flash evaporation phenomenon. In addition, the use of a valve to control the pressure drop in the flash chamber, will let us check its influence on NEF and thus on the time of flashing.

Acknowledgements

The authors gratefully acknowledge the financial support of the LEQUEUX Company.

References

- [1] H.K. Pulker, Flash evaporation, Vak. Forschung und Praxis (3) (2000) 197–198.
- [2] I. Aoki, Analysis of characteristics of water flash evaporation under low-pressure conditions, Heat Transfer – Asian Res. 29 (1) (2000) 22–33.
- [3] I. Aoki, Water flash evaporation under low pressure conditions, Heat Transfer – Jpn. Res. 23 (6) (1994) 544–555.
- [4] R. Peterson, S. Grewal, M. El-Wakil, Investigations of liquid flashing and evaporation due to sudden depressurization, Int. J. Heat Mass Transfer 27 (2) (1984) 301–310.
- [5] O. Miyatake, K. Murakami, Y. Kawata, T. Fujii, Fundamental experiments with flash evaporation, Heat Transfer – Jpn. Res. 2 (1973) 89–100.
- [6] O. Miyatake, T. Fujii, T. Tanaka, T. Nakaoka, Flash evaporation phenomena of pool water, Heat Transfer – Jpn. Res. 6 (1977) 13–24.
- [7] G. Gopalakrishna, V.M. Purushothaman, N. Lior, An experimental study of flash evaporation from liquid pools, Desalination 65 (1987) 139–151.
- [8] J. Kim, N. Lior, Some critical transitions in pool flash evaporation, Int. J. Heat Mass Transfer 40 (10) (1997) 2363–2372.
- [9] F. Massard, Aide-mémoire du thermicien, Elsevier, Amsterdam, 1997.